

Article

Twin Supersymmetric Dark Matter in Light of the First LZ Results

Marcin Badziak ^{1,*} , Giovanni Grilli di Cortona ^{2,3} , Keisuke Harigaya ^{4,5,6,7} and Michał Łukawski ¹

¹ Institute of Theoretical Physics, Faculty of Physics, University of Warsaw, ul. Pasteura 5, 02-093 Warsaw, Poland

² Istituto Nazionale di Fisica Nucleare, Sezione di Roma, Piazzale A. Moro 2, 00185 Roma, Italy

³ Istituto Nazionale di Fisica Nucleare, Laboratori Nazionali di Frascati, C.P. 13, 00044 Frascati, Italy

⁴ Department of Physics, University of Chicago, Chicago, IL 60637, USA

⁵ Enrico Fermi Institute, University of Chicago, Chicago, IL 60637, USA

⁶ Kavli Institute for Cosmological Physics, University of Chicago, Chicago, IL 60637, USA

⁷ Kavli Institute for the Physics and Mathematics of the Universe (WPI), The University of Tokyo Institutes for Advanced Study, The University of Tokyo, Kashiwa 277-8583, Chiba, Japan

* Correspondence: mbadziak@fuw.edu.pl

Abstract: We review the status of dark matter (DM) candidates in supersymmetric Twin Higgs models in light of the first results of the LUX-ZEPLIN (LZ) experiment. We found that, for twin bino-dominated DM, the new results strengthened the lower bound on the higgsino mass. However, a large part of the parameter space consistent with natural electroweak symmetry breaking is still allowed. In the case of twin-stau DM, the new results imply that, if the thermal abundance of the twin-stau LSP fits the observed density of DM, the twin stau cannot have a large left-handed component anymore.

Keywords: dark matter; supersymmetry; Twin Higgs



Citation: Badziak, M.; Grilli di Cortona, G.; Harigaya, K.; Łukawski, M. Twin Supersymmetric Dark Matter in Light of the First LZ Results. *Symmetry* **2023**, *15*, 386. <https://doi.org/10.3390/sym15020386>

Academic Editors: André Maeder and Vesselin G. Gueorguiev

Received: 30 December 2022

Revised: 24 January 2023

Accepted: 28 January 2023

Published: 1 February 2023



Copyright: © 2023 by the authors. Licensee MDPI, Basel, Switzerland. This article is an open access article distributed under the terms and conditions of the Creative Commons Attribution (CC BY) license (<https://creativecommons.org/licenses/by/4.0/>).

1. Introduction

Twin Higgs (TH) models [1] provide one of the best solutions to the little-hierarchy problem that stems from the lack of discovery of new coloured particles up to the energy scales probed by the LHC. In this class of models, the discovered Higgs boson is a pseudo-Nambu–Goldstone boson of an approximate global SU(4) symmetry. In order to avoid quadratically divergent contributions to the Higgs mass parameter from gauge and Yukawa interactions that explicitly break the SU(4) symmetry, a discrete \mathbb{Z}_2 , called twin symmetry, is introduced.

The twin symmetry interchanges the Standard Model (SM) particles with the corresponding twin particles, charged under twin gauge symmetry. In this setup, the twin top quark cancels the most dangerous quadratically divergent correction to the Higgs mass parameter from the SM top quark. Since the twin top quark is not charged under the SM gauge group, the LHC is not able to set any meaningful limits on its mass.

The twin symmetry alone, however, does not stabilize the SU(4) symmetry-breaking scale. Thus, the TH model requires UV completion that can be based, for example, on supersymmetry (SUSY) [2–8] or composite Higgs scenarios [9–12]. In the present paper, we focus on SUSY TH models. The twin symmetry in the supersymmetric framework implies the existence of many new particles that do not interact electromagnetically.

Hence, if the Lightest Supersymmetric Particle (LSP) resides in the twin sector, it may play a role of dark matter (DM) with very different features from the DM candidates in the Minimal Supersymmetric Standard Model (MSSM). A key difference between twin SUSY DM and the MSSM DM is that the former annihilates into twin states, and thus the relic abundance of twin SUSY DM is mostly unaffected by the structure of the visible sector.

This allows for disentangling the DM relic abundance from the DM-interaction rates with nucleons that are strongly constrained by direct-detection (DD) experiments. Due to the \mathbb{Z}_2 symmetry, a typical annihilation cross-section of twin SUSY DM is that of the weak interaction, and one may expect that the observed DM abundance is obtained for the LSP masses consistent with natural EW symmetry breaking.

While it is expected that the DD signal for twin SUSY DM is typically suppressed, it cannot be arbitrarily small if the TH mechanism is responsible for the solution to the hierarchy problem. This is because twin SUSY DM may still interact with nucleons via the mixing between the SM-like and twin Higgs bosons. This mixing is suppressed by the ratio v/v' , where v (v') is the SM (twin) Higgs vacuum expectation value, which is constrained by the LHC Higgs coupling measurements to be $v'/v \gtrsim 3$ [13]. The tuning of the EW scale grows as $(v'/v)^2$. Thus, for a given level of tuning of the EW scale, one expects a lower bound on the DD cross-section.

The two realizations of twin SUSY DM proposed in refs. [14,15] share the features described above (DM candidates have also been proposed in TH models without SUSY UV completion; see, e.g., refs. [16–29]). In Ref. [14], it was shown that twin neutralinos can be a natural DM candidate that avoid the shortcomings of the MSSM neutralino. On the other hand, in Ref. [15], the twin stau was shown to be a good DM candidate in the range of several hundred GeV without violating constraints on twin-stau self-interactions. Both DM candidates were shown to be consistent with the Xenon1T experiment [30] in the bulk of natural parameter space but with good prospects for detection at the LUX-ZEPLIN (LZ) experiment [31].

The main goal of this paper is to assess the impact of the recently published first LZ results [32], which are currently the strongest limits for DM masses above 10 GeV on twin neutralino and twin stau DM. We show that, despite excluding some part of the parameter space, both scenarios for twin SUSY DM can still accommodate a natural EW scale. Nevertheless, in some scenarios, the lower bound on v'/v becomes stronger than the bound from the LHC Higgs coupling measurements.

The rest of the paper is organized as follows. In Section 2, we analyse the case with a twin neutralino being the LSP. In Section 3, we focus on twin stau DM. Section 4 is devoted to our conclusions and final remarks.

2. Twin Neutralino DM

Let us begin with the case of a twin neutralino as a DM candidate. We assume an exact \mathbb{Z}_2 symmetry for the soft SUSY-breaking terms. The twin-neutralino sector consists of four states: bino, wino and two higgsinos. It is governed by five free parameters. The masses of pure higgsinos, bino and wino are given by μ , M_1 and M_2 , respectively. The mixing between twin neutralinos is governed by $\tan\beta$ and the vacuum expectation value (VEV) of the twin Higgs boson, v' . The mixing between MSSM and twin neutralinos is suppressed and can be safely neglected in the computation of the relic abundance and direct-detection cross section.

In the following, we assess the impact of the new LZ results on twin-neutralino DM. Following Ref. [14], we focus on a case in which the wino is decoupled and the Lightest Supersymmetric Particle (LSP) is dominated by the bino component. The naturalness of SUSY TH models requires the supersymmetric higgsino mass parameter to be smaller than about 1.5 TeV, which inevitably leads to some non-negligible twin-higgsino component of the LSP. The bino-higgsino mixing is proportional to the Higgs VEV, which is larger in the twin sector. As a consequence, the twin bino-like neutralino is generically lighter than the bino-like neutralino.

In the MSSM, if the bino-like neutralino is the LSP, the correct relic abundance is obtained only for fine-tuned regions of the parameter space, where s-channel resonances or coannihilations are very efficient [33–35]. The freeze-out of the bino is controlled by the $\tilde{B}\tilde{B} \rightarrow f\bar{f}$ process mediated by t-channel sfermion exchange, whose s-wave amplitude is chirality-suppressed for $m_f \ll M_1$.

The cross section of the p-wave annihilation scales as M_1^2/m_f^4 . LEP lower bounds on sfermion masses translate to upper limits on this cross section, which necessarily lead to overproduction of the bino.

However, in twin supersymmetry, the masses of the twin fermions may be large enough to avoid chirality suppression. In fact, they are larger by a factor of v'/v due to the \mathbb{Z}_2 breaking in potential. Nevertheless, in order to have m_f of order M_1 , we need to break the \mathbb{Z}_2 symmetry in the Yukawa sector as well. This is favourable from a cosmological point of view because the \mathbb{Z}_2 breaking in the Yukawa sector relaxes the ΔN_{eff} problem [20,21] and allows for first-order phase transition in TH models [36]. In the following, we consider a twin neutralino as a candidate for DM.

We consider the effect of a light stau on the relic abundance [14], motivated by the fact that staus are the least constrained sfermion. Indeed, the LEP bound on the mass of the stau reads $m_{\tilde{\tau}} \gtrsim 90$ GeV [37–40]. The LHC constraints on the direct production of staus are still rather weak; however, some range of parameter space with the left-handed stau mass above the LEP bound is excluded [41]. Since the LHC constraints on direct production of the right-handed stau are essentially absent, we consider a purely right-handed stau, $\tilde{\tau} \simeq \tilde{\tau}_R$, with the left-handed component decoupled.

For the calculation of the relic abundance of the twin neutralino, we use Micromegas [42–44]. We adjusted the MSSM implementation by changing v to v' , so that the masses and decay widths of particles in the twin sector are appropriately rescaled. In this way, the coannihilation within each sector is included. However, we neglect coannihilation between twin neutralino and the MSSM states since its impact on the relic abundance is typically small [14].

First, in Figure 1, we consider the μ - M_1 plane. The mass of the stau is adjusted so that, in every point of the parameter space, $\Omega h^2 = 0.12$. The purple-coloured region has $m_{\tilde{\tau}} < 90$ GeV and is excluded by LEP. The orange- and green-shaded regions show the DD bounds from Xenon1T and LZ, respectively. The interactions between twin neutralinos and nuclei are mediated by the Higgs boson. We use the default Micromegas’ values of the nucleon form factors that can be found in Table 3 of Ref. [45]. The effective interaction between the bino-like neutralino and the Higgs boson is given by [46]

$$c_{h\tilde{B}'\tilde{B}'} \simeq \frac{g_1^2 v'}{2\sqrt{2}\mu} \left(s_{2\beta} + \frac{M_1}{\mu} \right) \frac{v}{v'} \tag{1}$$

where v/v' is the factor coming from the Higgs-twin Higgs mixing. Interestingly, the $1/v'$ factor cancels against the v' in the twin bino-higgsino mixing, and the dependence on the VEV of the twin Higgs vanishes in first approximation. This coupling becomes small for large μ , and the contribution proportional to $\sin 2\beta$ vanishes in the limit of large $\tan \beta$.

The twin Higgs mechanism allows for larger values of μ , which is expected to be around the $SU(4)$ -breaking scale $f \equiv \sqrt{v^2 + v'^2}$, without much tuning [5]. For large M_1 , the Xenon1T bound in Figure 1 requires $\mu \gtrsim 600$ GeV, while LZ sets a lower bound $\mu \gtrsim 900$ GeV. For the smallest neutralino mass compatible with the LEP results, $M_1 \simeq 60$ GeV, the bound is the strongest and gives $\mu > 700$ GeV and $\mu > 1200$ GeV from Xenon1T and from LZ, respectively. The predicted sensitivity of LZ will probe this scenario up to $\mu \simeq 3$ TeV.

Blue contours correspond to $m_{\tilde{\tau}}$, which reproduces the observed relic abundance. There is a resonant suppression in the relic density at the DM mass $m_{DM} = 0.5 m_{Z'} \approx 135$ GeV from the s-channel annihilation through Z' into twin fermions, which has been neglected in previous work. Since the coupling of the neutralino to Z' is proportional to $1/\mu^2$ [46], the correct relic abundance is obtained for larger values of μ .

There should be a Higgs resonance at $m_{DM} = 0.5 m_h = 62.5$ GeV, shown as a thick, dashed contour. We do not include this resonance in our computation of the relic density, since it significantly affects the abundance only within a few hundred MeV range of the DM masses around the centre of the resonance.

Hence, the LSP mass would have to be fine-tuned at a level of one percent. This is in contrast to the Z' resonance, which is wide and effective for a wide range of the DM masses between about 125 and 145 GeV.

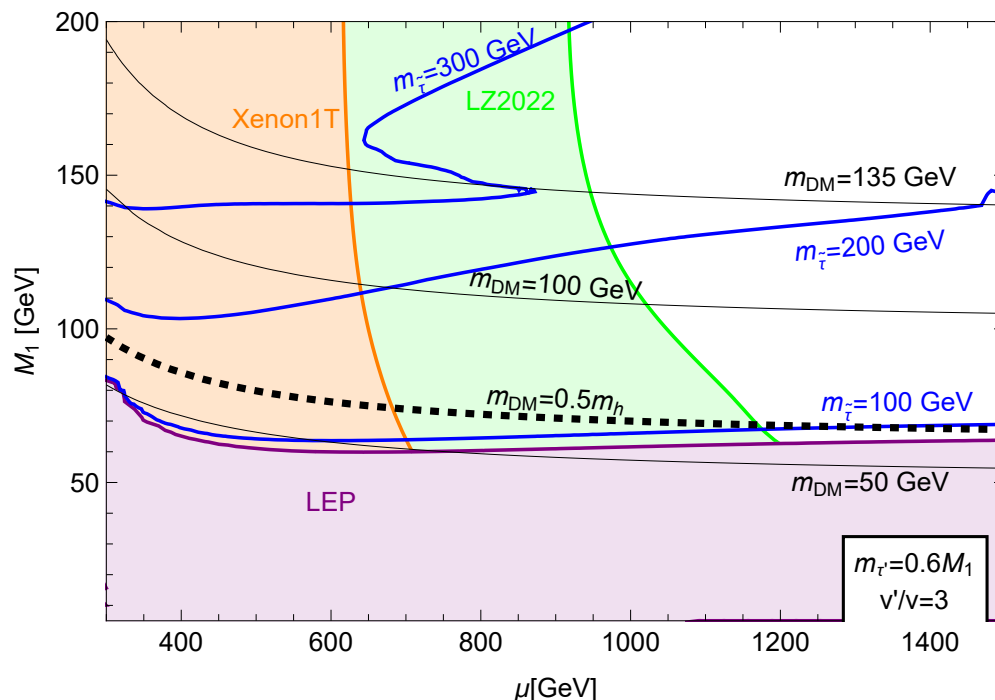


Figure 1. The plot of the μ - M_1 plane with contours of the stau mass, $m_{\tilde{\tau}} = 100, 200, 300$ GeV, reproducing correct relic abundance $\Omega h^2 = 0.12$ for $\tan \beta = 5$, $m_{\tau'} = 0.6 M_1$ and $v'/v = 3$. The LEP constraint on the stau mass is shown by a purple-coloured region. The orange region is excluded by the Xenon1T experiment [30], and the green region is excluded by the new LZ results [32]. Black contours show the mass of the twin neutralino, while the thick dashed curve corresponds to $m_{DM} = 0.5 m_h$.

Figure 2 shows the parameter space in the M_1 - $\tan \beta$ plane with $\mu = 1$ TeV, $m_{\tau'} = 0.6 M_1$ and $v'/v = 3$. Once again, the blue contours correspond to different values of the stau mass reproducing the correct relic abundance. The Z' resonance at $m_{DM} = 0.5 m_{Z'} = 135$ GeV significantly boosts the twin-neutralino annihilation cross section, and the correct relic abundance is obtained for a larger stau mass for fixed $\tan \beta$. Since the bino- Z coupling is proportional to $\cos 2\beta$ [46], for fixed $m_{\tilde{\tau}}$, the correct relic abundance in the resonance region is obtained for smaller values of $\tan \beta$ with respect to the case far away from the resonance region. Once again, we neglect the Higgs resonance in our results but acknowledge its position as a thick dashed line at $m_{DM} = 0.5 m_h$.

The DD bound weakens with increasing $\tan \beta$, as the first term in Equation (1) vanishes in the large- $\tan \beta$ limit. The plot also shows that the lower limit on $\tan \beta$ becomes weaker for larger M_1 . This is because the upper bounds on the DD cross section from LZ are weaker for larger DM masses (above a few tens of GeV). The limit on $\tan \beta$ decreases from about 7 to 4 when the LSP mass increases from 50 to 200 GeV.

Figure 3 shows the μ - $\tan \beta$ plane fixing $M_1 = 100$ GeV, $m_{\tau'} = 0.6 M_1$ and $v'/v = 3$. Since we have chosen $M_1 = 100$ GeV, the correct relic abundance is obtained for a relatively heavy twin stau, and the LEP bound on the mass of the stau is absent. We show the current (green) and predicted (cyan) sensitivity of the LZ experiment.

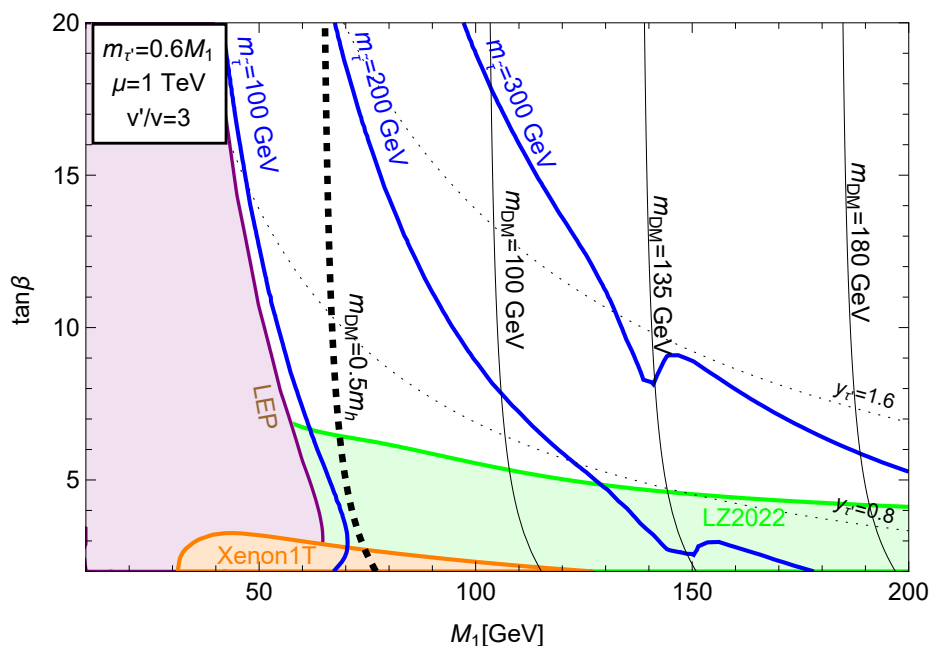


Figure 2. The plot of M_1 - $\tan\beta$ plane with contours of the stau mass, $m_{\tilde{\tau}} = 100, 200, 300$ GeV, reproducing the correct relic abundance $\Omega h^2 = 0.12$ for $\mu = 1$ TeV, $m_{\tau'} = 0.6M_1$ and $v'/v = 3$. The LEP constraint on the stau mass is shown by a purple-coloured region. The orange region is excluded by the Xenon1T experiment [30], and the green region is excluded by the new LZ results [32]. Black contours show the mass of the twin neutralino, while the thick, dashed curve corresponds to $m_{DM} = 0.5m_h$.

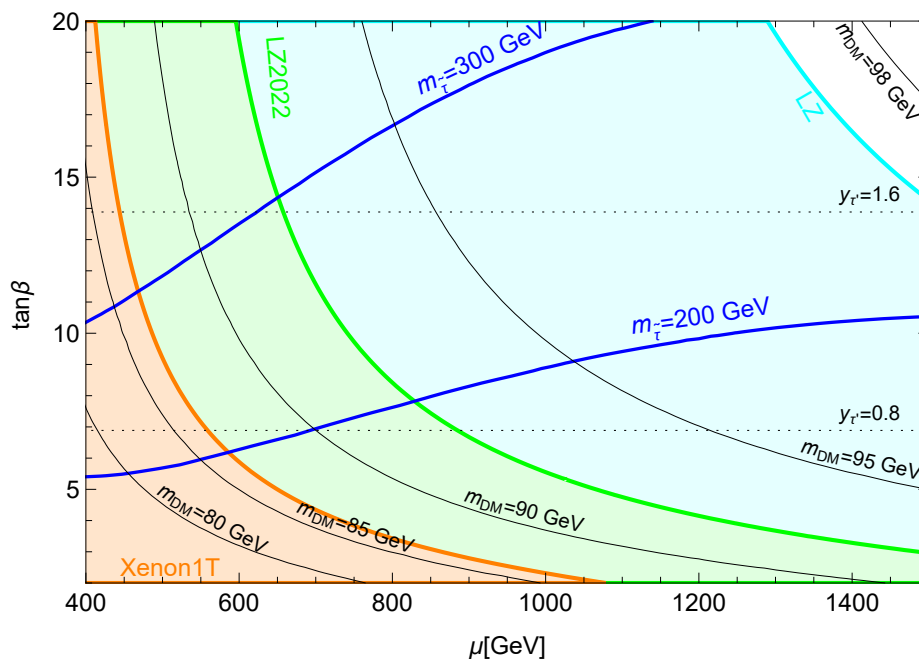


Figure 3. The plot of the μ - $\tan\beta$ plane with contours of the stau mass, $m_{\tilde{\tau}} = 200, 300, 400, 500$ and 600 GeV, reproducing the correct relic abundance $\Omega h^2 = 0.12$ for $M_1 = 100$ GeV, $m_{\tau'} = 0.6M_1$ and $v'/v = 3$. The LEP constraint on the stau mass is outside the plotted region. The orange region is excluded by the Xenon1T experiment [30], and the green region is excluded by the new LZ results [32]. The predicted sensitivity of LZ corresponds to the cyan region. Black solid lines correspond to the mass of the LSP.

The DD bounds on μ strongly depend on $\tan\beta$; at large $\tan\beta$, the constraint on μ can be relaxed. Even though μ in SUSY TH models is natural up to $\mu \simeq f$, the results of LZ with the full exposure probe a large portion of the parameter space. The current constraints from LZ for $\tan\beta = 5$ exclude $\mu \lesssim 1050$ GeV; however, for $\tan\beta = 10$, only $\mu \lesssim 750$ GeV is excluded. $\tan\beta$ cannot be arbitrarily large because it would lead to non-perturbatively large twin tau Yukawa coupling, which is proportional to $1/\cos(\beta)$. Due to the breaking of \mathbb{Z}_2 in Yukawa couplings, the perturbativity bound on $\tan\beta$ is much stronger than in the MSSM.

For $m_{\tau'} = 60$ GeV, set in Figure 3, $\tan\beta = 7$ (14) corresponds to twin tau Yukawa couplings of 0.8 (1.6) for which the Landau pole is avoided up to about 10^{16} (10^4) GeV assuming MSSM renormalization group equations. However, if tau is charged under an extra gauge interactions with large gauge coupling, which is an essential ingredient in SUSY D-term TH models [5–7], twin tau Yukawa can decrease with increasing energy scales, which would strongly relax the upper bound on $\tan\beta$ from perturbativity. In such a scenario, even $\tan\beta = 20$ may not result in a Landau pole at low energy scales for which LZ excludes $\mu \lesssim 600$ GeV.

LZ with full exposure should probe large values of μ . In the case of null results, this suggests that large $\tan\beta$ is preferred in this scenario due to naturalness. For $\tan\beta = 20$, values of μ will be probed by LZ only up to about 1.3 TeV.

3. Twin Stau DM

In the SUSY TH model, the couplings are fixed by the \mathbb{Z}_2 symmetry. The relic abundance is determined mostly by the spectrum of the theory, which we parametrize by soft supersymmetry-breaking parameters, similarly to the MSSM. The mass matrix of the twin stau is given by

$$m_{\tilde{\tau}'}^2 = \begin{pmatrix} m_{3L}^2 + \Delta_{\tilde{\tau}'_L} + m_{\tau'}^2 & v'(A_\tau - \mu y_{\tau'} \sin(\beta)) \\ v'(A_\tau - \mu y_{\tau'} \sin(\beta)) & m_{3R}^2 + \Delta_{\tilde{\tau}'_R} + m_{\tau'}^2 \end{pmatrix}, \quad (2)$$

while the mass matrix for the MSSM stau is obtained by removing the primes from the above formula. Throughout the paper, we assume that there is no \mathbb{Z}_2 breaking in soft SUSY-breaking terms—that is, $m_{3L} = m_{3L'}$ and $m_{3R} = m_{3R'}$. We also implicitly assume equal higgsino mass terms for the MSSM and twin sector as well. Moreover, without much loss of generality, we set the soft trilinear couplings $A_{\tau'} = A_\tau = 0$.

The reason is that their effects are similar to the relevant part of the off-diagonal entry $\mu v' y_{\tau'} \sin(\beta)$, and thus we can always mimic that term by adjusting μ , $\tan\beta$ and v' . In the minimal setup, there is no need for \mathbb{Z}_2 breaking in the Yukawa sector and $y_{\tau'} = y_\tau$. The D-term contributions to left- and right-handed twin staus are $\Delta_{\tilde{\tau}'_L} = (-1/2 + \sin^2\theta_W) m_Z^2 \cos 2\beta$ and $\Delta_{\tilde{\tau}'_R} = -m_Z^2 \sin^2\theta_W \cos 2\beta$, where θ_W is the Weinberg angle and $m_{Z'}$ is the mass of the Z' boson. Note that, for $\tan\beta > 1$, the D-term contributions are positive for both left-handed and right-handed staus. Thus, the gauge contributions are larger in the twin sector since $v'/v \gtrsim 3$ is required by the LHC Higgs coupling measurements.

We assume that the twin electromagnetism is unbroken; hence, the twin stau has long-range self-interactions mediated by the twin photon. Such interactions are constrained by the ellipticity measurements on DM halos. Large self-interactions of the DM lead to isotropization of the velocity distribution, which, in turn, leads to faster decrease of the ellipticity. For the twin electromagnetic gauge coupling equal to the SM one, the bound is $m_{\tilde{\tau}'} \gtrsim 210$ GeV [47].

We compute the relic abundance of the twin stau with our modified version of Micromegas. Since, in some parts of the parameter space, the mass splitting between the MSSM stau and twin stau is very small, we include the coannihilation of the LSP with stau using the procedure detailed in Ref. [15].

First, we consider the case of minimal tuning, which is achieved for the smallest $v'/v = 3$ allowed by the Higgs coupling measurements. Figure 4 corresponds to the left panel of Figure 5 in Ref. [15] with updated direct detection bound from LZ.

There are roughly four regions where the twin stau is not the LSP. As a result of the absence of \mathbb{Z}_2 breaking in the SUSY-breaking terms, small mixing leads to stau LSP or twin sneutrino LSP (red regions). The former happens because, for mostly right-handed stau $\tilde{\tau}'_1$, the diagonal entries dominate the mass matrix, and the MSSM stau is lighter due to a positive D -term contribution for staus. On the other hand, in the region where the stau is mostly left-handed, the twin sneutrino is the LSP because the D -term contribution to the sneutrino mass squared is negative. Furthermore, for small soft stau masses, $\tilde{\tau}'$ becomes tachyonic due to the large off-diagonal terms (the purple region). Finally, for $\mu = M_1 = 700$ GeV, the lightest MSSM neutralino has a mass of $m_{\tilde{N}_1} \simeq 600$ GeV, and it becomes the LSP when m_{3R} and m_{3L} are larger than about 600 GeV (the brown region).

The twin bino mediates t - and u -channel $\tilde{\tau}'\tilde{\tau}' \rightarrow \tau'\tau'$ processes, which, for light \tilde{B}' , become dominant in the twin stau freeze-out. As a result, the mass of the twin stau $m_{\tilde{\tau}'}$ reproducing the correct relic abundance (blue curve) is boosted to values between 450 and 500 GeV, as compared to the case with a heavy bino that we will discuss later.

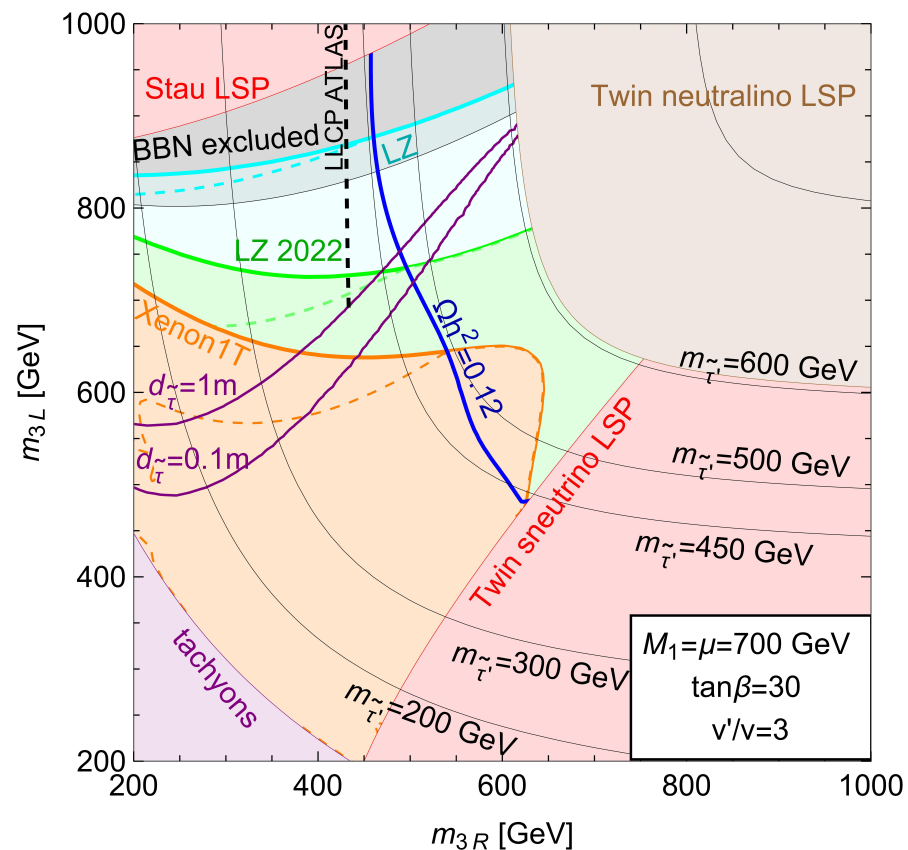


Figure 4. Contours of the twin-stau thermal abundance $\Omega_{\tilde{\tau}'}^{\text{th}} h^2 = 0.12$ (blue) and twin stau masses (black) for $\mu = M_1 = 700$ GeV, $\tan\beta = 30$ and $v'/v = 3$ in the plane $m_{3R} - m_{3L}$. The orange and green region denotes the area excluded by Xenon1T [30] and the new LZ results [32] (cyan shows the expected sensitivity of LZ with the full exposure [31]), assuming that the twin stau abundance $\Omega_{\tilde{\tau}'} h^2 = 0.12$ in every point of the plane. The dashed curves instead assume the scaling of the bound with the thermal abundance if $\Omega_{\tilde{\tau}'} h^2 = \Omega_{\tilde{\tau}'}^{\text{th}} h^2 < 0.12$, which corresponds to the case in which the twin stau is only a sub-component of the total DM. The BBN-excluded region is gray, while the parameter space with a tachyonic twin stau is purple. In the red region, the twin sneutrino or stau is the LSP, and in the brown region, the twin neutralino is the LSP. The decay length contours of the stau $d_{\tilde{\tau}'} = 1, 0.1$ m are purple. The black dashed line labelled LLCP ATLAS is a contour for $m_{\tilde{\tau}'} = 430$ GeV, which is a lower bound for long-lived stau ($d_{\tilde{\tau}'} > 1$ m).

Relatively light staus could be produced in colliders and observed as either a long-lived particle (for the stau decay length $d_{\tilde{\tau}} \gtrsim 1$ m) or a disappearing charged track ($10 \text{ cm} \lesssim d_{\tilde{\tau}} \lesssim 1$ m) [48]. This region is shown in Figure 4 by two purple solid curves. In the minimal scenario, the decay of the stau is mediated by bino-higgsino-twin higgsino-twin bino mixing. Higgsino-twin higgsino mixing is obtained by integrating out heavy degrees of freedom and, in principle, is UV-dependent. We found that the decay length is approximately given by

$$d_{\tilde{\tau}} \simeq 2.7 \text{ m} \left(\frac{m_{\tilde{\tau}}}{300 \text{ GeV}} \right)^2 \left(\frac{M}{10^6 \text{ GeV}} \right)^2 \left(\frac{10 \text{ GeV}}{m_{\tilde{\tau}} - m_{\tilde{\tau}'}} \right)^5 \quad (3)$$

where $1/M$ is the effective coupling of the $d = 5$ operator $\tilde{\tau}\tilde{\tau}'^\dagger\tau^\dagger\tau'$. The reference value of M can be obtained in D-term SUSY twin Higgs models; see Ref. [15] for details. Those results provide the upper limit on the stau decay length and could be altered by an $\mathcal{O}(1)$ factor in specific UV completion. It should be noted that even small bino-twin bino mass mixing could enhance the stau decay and hide the signal [15].

For a very small mass splitting between the stau and the twin stau, the stau becomes too long-lived and causes cosmological problems. For nearly degenerate cases, the stau decays after the BBN and spoils the nuclei primordial abundance. In Figure 4, the BBN bound is shown by a coloured gray region and corresponds to the region in which the decay channel $\tilde{\tau} \rightarrow \tilde{\tau}'\tau\tau'^\dagger$ is kinematically closed, $m_{\tilde{\tau}} < m_{\tilde{\tau}'} + m_\tau + m_{\tau'}$.

Disappearing charged track searches exclude staus with masses below about 200 GeV [49], which corresponds to underproduction of the twin-stau LSP. This search does not really constrain this scenario, since the bound on DM self-interactions already sets the lower limit on the mass of the twin stau $m_{\tilde{\tau}}' \gtrsim 210$ GeV but may become relevant when the LHC collects more data.

A long-lived right-handed stau with the decay length above $d_{\tilde{\tau}} \gtrsim \mathcal{O}(1)$ m is excluded for masses up to 430 GeV [50]. Since, in a significant portion of the parameter space, the stau can be a long-lived particle, we also include a contour of the stau mass $m_{\tilde{\tau}} = 430$ GeV in Figure 4 indicating the current ATLAS bound (black dashed curve). It is clear that, for the twin stau saturating the DM relic abundance, the long-lived stau is allowed by the LHC data. However, it must be stressed that this is the case due to a light bino, which boosts stau masses reproducing $\Omega^{\text{th}}h^2 = 0.12$ above 450 GeV.

We will elaborate on the effect of a light bino when we discuss the effect of the $SU(4)$ -breaking scale on the parameter space. Still, long-lived-particle searches do constrain the scenario in which the thermally produced twin stau is only a fraction of the observed DM, $\eta \equiv \Omega^{\text{th}}h^2/0.12$. For mostly right-handed stau DM, it sets the lower bound on the twin stau fraction of the observed DM between $\eta \approx 0.75$ for $m_{3L} \approx 700$ GeV (lowest value satisfying both $d_{\tilde{\tau}} > 1$ m and new LZ results) and $\eta \approx 0.9$ for $m_{3L} \approx 820$ GeV (largest value satisfying the BBN constraint).

Xenon1T has already excluded the case of maximally mixed twin stau DM, probing masses up to 550 GeV. New limits on DD cross-sections from LZ [32] exclude the whole region characterized by a large left-handed component of the twin stau including the one in which the twin-stau thermal abundance is too large but $\Omega_{\tilde{\tau}'}h^2 = 0.12$ is obtained assuming late entropy injection. While it may seem from the plot that one needs to go into a very specific part of the parameter space, it should be kept in mind that $v'/v = 3$ is the lowest value allowed by the Higgs coupling measurements. Since the interaction of the twin stau with nucleons is mediated by the Higgs portal, larger ratios of VEVs v'/v can substantially weaken those bounds.

Figure 5 presents the results of varying v'/v to show the effect of high scale $SU(4)$ breaking. We set $m_{3R} = m_{3L} - 600$ GeV so that the twin stau is mostly right-handed. We consider two qualitatively different cases of light and heavy bino.

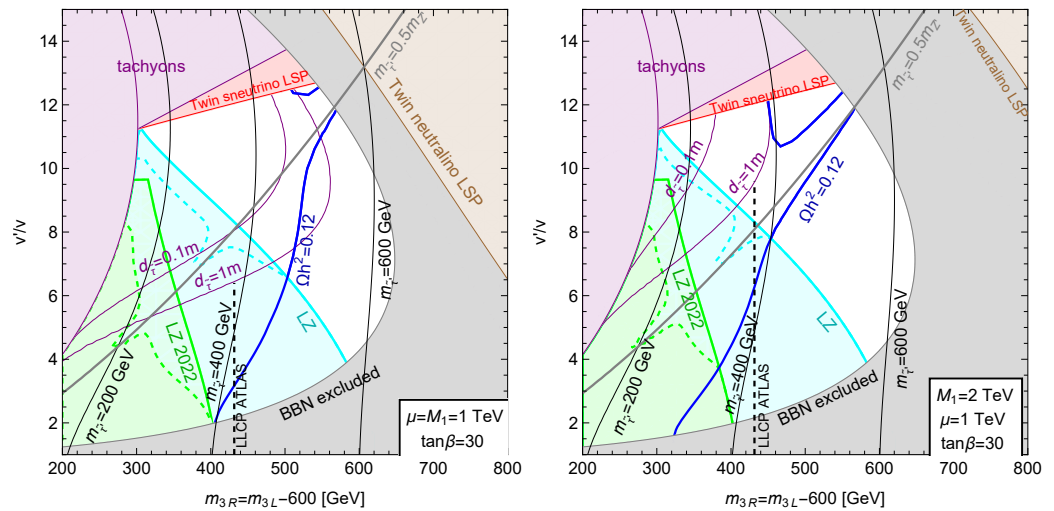


Figure 5. The same as in Figure 4 but in the $m_{3R} - v'/v$ plane for $m_{3R} = m_{3L} - 600$ GeV, $\mu = 1$ TeV, $\tan \beta = 30$ and a light bino with $M_1 = 1$ TeV (left panel) or a heavy bino with $M_1 = 2$ TeV (right panel).

For large v'/v and $m_{3R} \lesssim 300$ GeV, the off-diagonal stau mass term dominates, and the twin stau becomes tachyonic. Since the mass splitting between the twin sneutrino and the left-handed twin stau is set by $m_{Z'}$, v'/v cannot be too large also for $m_{3R} \gtrsim 300$ GeV, otherwise the twin sneutrino would be the LSP or even tachyonic.

Interestingly, the BBN constraint also provides an upper bound on m_{3R} since increasing m_{3R} reduces the mass splitting between the stau and twin stau. Moreover, the BBN constraint also sets an upper bound on v'/v . This is because, in the limit of large v' , the D -term contribution to the twin stau mass that is proportional to v'^2 dominates over the \mathbb{Z}_2 -symmetric contribution from soft SUSY breaking.

Since the off-diagonal term in the twin stau mass matrix, which tends to decrease the twin stau mass, grows only linearly with v' and cannot compensate the increase of the twin stau mass due to the D -term, the mass difference between the twin stau and stau decreases leading to the BBN exclusion for large v' . All in all, for the parameters used in Figure 5, the twin stau can be the LSP without violating the BBN constraint only if $v'/v \lesssim 12$.

Figure 5 demonstrates that increasing v' leads not only to suppressed DD cross-section but also to larger stau masses compatible with $\Omega^{\text{th}} h^2 = 0.12$. This is because, for small v'/v , the mass splitting between the stau and twin stau is small, and coannihilations efficiently enhance the relic abundance (for a fixed LSP mass) so that a smaller twin stau mass is required to match the observed DM density.

As mentioned before, a light bino significantly increases the annihilation rate of the twin stau. As a result, the twin stau is kept in equilibrium longer, freezing out with a lower abundance. Moreover, since the decay of the stau is mediated by the coupling to the bino and by higgsino mixing, a light bino necessarily means that the stau decay length becomes shorter.

In the case of a light bino with $M_1 = 1$ TeV, presented in the left panel of Figure 5, correct relic abundance is achieved for twin stau masses between about 400 GeV for $v'/v \approx 3$ up to about 500 GeV for $v'/v \approx 10$. Notice also that, for v'/v between about 10 and 12 at $m_{\tilde{\tau}'} \approx 0.5m_{Z'}$, resonant annihilation into twin fermions is very efficient, leading to $\Omega^{\text{th}} h^2 = 0.12$ even above 500 GeV; however, much larger values are not possible due to the BBN constraint. While a large part of the parameter space has the stau decay length above 1 m, the $\Omega^{\text{th}} h^2 = 0.12$ contour lies above $m_{\tilde{\tau}} = 430$ GeV for $v'/v \gtrsim 3$, and hence the current constraints from the ATLAS searches for long-lived charged particles are not stronger than those from the Higgs couplings measurements. As expected from Figure 4, the new results of the LZ experiment do not constrain the twin stau LSP with a large fraction of the right-handed component for $v'/v > 3$.

However, the expected sensitivity of LZ can probe the thermal twin stau DM up to $v'/v \simeq 6.5$, which would correspond to 5% fine-tuning in the case of null results. In the case of a heavy twin bino with $M_1 = 2$ TeV, as shown in the right panel of Figure 5, the correct relic abundance is obtained for twin stau masses between about 350 GeV for $v'/v \approx 3$ and up to about 400 GeV in the limit of large v' , except for the region with the twin stau resonant annihilation via Z' exchange where the twin stau mass can exceed 500 GeV and is limited only by the BBN constraints, similarly as in the light bino case.

The heavy bino increases the lifetime of the stau, so that all parameter space with the correct relic abundance also has $d_{\tilde{\tau}} > 1$ m. Considering this, the ATLAS search for long-lived particles set a lower bound $v'/v \gtrsim 6$ assuming twin stau thermal DM. The expected sensitivity of LZ probes values of v'/v up to about 8 in the thermal scenario, which, in the case of null results, would correspond to fine-tuning of about 3%.

It is noteworthy that the mostly right-handed twin stau DM is currently more constrained by the ATLAS search for long-lived charged particles than by the new LZ results. However, the full sensitivity of the LZ experiment will probe large parts of the parameter space with $m_{\tilde{\tau}} > 430$ GeV, which is currently unconstrained by the LHC.

4. Conclusions

We analysed the implications of the new LZ results on supersymmetric twin dark matter. We considered a twin neutralino and a twin stau as candidates for DM.

In the scenario of the twin-neutralino LSP, the new LZ bound sets a lower limit on the higgsino mass parameter μ , which is related to the naturalness of the model. This bound depends on $\tan\beta$ and M_1 . We demonstrated the constraint from the new LZ results for benchmark parameters corresponding to the previous analysis of Ref. [14]. Moreover, we presented the interplay between μ and $\tan\beta$ on the prospects of direct detection of the twin-neutralino DM.

For $\tan\beta = 5$, the new LZ results excluded $\mu \lesssim 1$ TeV for the DM mass of about 100 GeV; however, this bound could be relaxed to $\mu \lesssim 600$ GeV for $\tan\beta = 20$. These results are not in tension with naturalness, since one naturally expects that $\mu \sim f$, and thus $\mu \approx 1$ TeV does not induce tuning worse than 10%. The LZ is expected to strengthen these bounds with the full dataset expected in a few years. For $\tan\beta = 5$, it could exclude μ up to 3 TeV, which is disfavoured by naturalness. However, for large $\tan\beta = 20$, those limits could be as low as $\mu > 1.3$ TeV.

In the twin-stau LSP scenario, the new LZ results exclude a large left-handed component of the twin stau LSP. The DD cross-section in this case strongly depends on the ratio v'/v and could be substantially reduced for larger $SU(4)$ -breaking scales. We demonstrated the updated DD bounds from LZ for the benchmark parameters analysed in Ref. [15]. Moreover, in Figure 5, we explicitly showed the impact of varying v'/v on the parameter space in cases of light and heavy bino. We analysed in depth the interplay between the searches for long-lived charged particles and the current and future constraints from LZ. The LZ experiment with the full dataset will probe parts of the parameter space that are yet unavailable for collider searches.

Let us end with a general remark that, while complete exclusion of these scenarios seems unlikely in the near future, the LZ experiment is expected to probe the most natural part of the parameter space. Thus, we should learn in the coming years whether twin supersymmetry can simultaneously explain the EW scale and provide the solution to the DM puzzle.

Author Contributions: Conceptualization, M.B., G.G.d.C., K.H. and M.Ł.; Analysis, M.B., G.G.d.C., K.H. and M.Ł.; Writing, M.B., G.G.d.C., K.H. and M.Ł.; All authors have read and agreed to the published version of the manuscript.

Funding: This work was partially supported by the National Science Centre, Poland, under research grant no. 2020/38/E/ST2/00243.

Conflicts of Interest: The authors declare no conflict of interest.

References

1. Chacko, Z.; Goh, H.S.; Harnik, R. The Twin Higgs: Natural electroweak breaking from mirror symmetry. *Phys. Rev. Lett.* **2006**, *96*, 231802. [[CrossRef](#)]
2. Falkowski, A.; Pokorski, S.; Schmaltz, M. Twin SUSY. *Phys. Rev. D* **2006**, *74*, 035003. [[CrossRef](#)]
3. Chang, S.; Hall, L.J.; Weiner, N. A Supersymmetric twin Higgs. *Phys. Rev. D* **2007**, *75*, 035009. [[CrossRef](#)]
4. Craig, N.; Howe, K. Doubling down on naturalness with a supersymmetric twin Higgs. *J. High Energy Phys.* **2014**, *03*, 140. [[CrossRef](#)]
5. Badziak, M.; Harigaya, K. Supersymmetric D-term Twin Higgs. *J. High Energy Phys.* **2017**, *06*, 65. [[CrossRef](#)]
6. Badziak, M.; Harigaya, K. Minimal Non-Abelian Supersymmetric Twin Higgs. *J. High Energy Phys.* **2017**, *10*, 109. [[CrossRef](#)]
7. Badziak, M.; Harigaya, K. Asymptotically Free Natural Supersymmetric Twin Higgs Model. *Phys. Rev. Lett.* **2018**, *120*, 211803. [[CrossRef](#)]
8. Katz, A.; Mariotti, A.; Pokorski, S.; Redigolo, D.; Ziegler, R. SUSY Meets Her Twin. *J. High Energy Phys.* **2017**, *1*, 142. [[CrossRef](#)]
9. Batra, P.; Chacko, Z. A Composite Twin Higgs Model. *Phys. Rev. D* **2009**, *79*, 095012. [[CrossRef](#)]
10. Geller, M.; Telem, O. Holographic Twin Higgs Model. *Phys. Rev. Lett.* **2015**, *114*, 191801. [[CrossRef](#)]
11. Barbieri, R.; Greco, D.; Rattazzi, R.; Wulzer, A. The Composite Twin Higgs scenario. *J. High Energy Phys.* **2015**, *08*, 161. [[CrossRef](#)]
12. Low, M.; Tesi, A.; Wang, L.T. Twin Higgs mechanism and a composite Higgs boson. *Phys. Rev. D* **2015**, *91*, 095012. [[CrossRef](#)]
13. Ahmed, A. Heavy Higgs of the Twin Higgs Models. *J. High Energy Phys.* **2018**, *02*, 048. [[CrossRef](#)]
14. Badziak, M.; Grilli Di Cortona, G.; Harigaya, K. Natural Twin Neutralino Dark Matter. *Phys. Rev. Lett.* **2020**, *124*, 121803. [[CrossRef](#)]
15. Badziak, M.; Grilli di Cortona, G.; Harigaya, K.; Łukawski, M. Charged dark matter in supersymmetric twin Higgs models. *J. High Energy Phys.* **2022**, *10*, 057. [[CrossRef](#)]
16. Farina, M. Asymmetric Twin Dark Matter. *J. Cosmol. Astropart. Phys.* **2015**, *1511*, 017. [[CrossRef](#)]
17. Prilepina, V.; Tsai, Y. Reconciling Large Furthermore, Small-Scale Structure In Twin Higgs Models. *J. High Energy Phys.* **2017**, *09*, 033. [[CrossRef](#)]
18. Chacko, Z.; Curtin, D.; Geller, M.; Tsai, Y. Direct detection of mirror matter in Twin Higgs models. *J. High Energy Phys.* **2021**, *11*, 198. [[CrossRef](#)]
19. Beauchesne, H.; Kats, Y. Cosmology of the Twin Higgs without explicit \mathbb{Z}_2 breaking. *J. High Energy Phys.* **2021**, *12*, 160. [[CrossRef](#)]
20. Barbieri, R.; Hall, L.J.; Harigaya, K. Minimal Mirror Twin Higgs. *J. High Energy Phys.* **2016**, *11*, 172. [[CrossRef](#)]
21. Barbieri, R.; Hall, L.J.; Harigaya, K. Effective Theory of Flavor for Minimal Mirror Twin Higgs. *J. High Energy Phys.* **2017**, *10*, 015. [[CrossRef](#)]
22. Craig, N.; Katz, A.; Strassler, M.; Sundrum, R. Naturalness in the Dark at the LHC. *J. High Energy Phys.* **2015**, *07*, 105. [[CrossRef](#)]
23. Curtin, D.; Gryba, S.; Setford, J.; Hooper, D.; Scholtz, J. Resurrecting the Fraternal Twin WIMP Miracle. *arXiv* **2021**, arXiv:2106.12578.
24. Terning, J.; Verhaaren, C.B.; Zora, K. Composite Twin Dark Matter. *Phys. Rev.* **2019**, *D99*, 095020. [[CrossRef](#)]
25. Hochberg, Y.; Kuflik, E.; Murayama, H. Twin Higgs model with strongly interacting massive particle dark matter. *Phys. Rev.* **2019**, *D99*, 015005. [[CrossRef](#)]
26. Cheng, H.C.; Li, L.; Zheng, R. Coscattering/Coannihilation Dark Matter in a Fraternal Twin Higgs Model. *J. High Energy Phys.* **2018**, *09*, 098. [[CrossRef](#)]
27. Freytsis, M.; Knapen, S.; Robinson, D.J.; Tsai, Y. Gamma-rays from Dark Showers with Twin Higgs Models. *J. High Energy Phys.* **2016**, *05*, 018. [[CrossRef](#)]
28. Craig, N.; Katz, A. The Fraternal WIMP Miracle. *J. Cosmol. Astropart. Phys.* **2015**, *1510*, 054. [[CrossRef](#)]
29. Garcia Garcia, I.; Lasenby, R.; March-Russell, J. Twin Higgs Asymmetric Dark Matter. *Phys. Rev. Lett.* **2015**, *115*, 121801. [[CrossRef](#)]
30. Aprile, E.; Aalbers, J.; Agostini, F.; Alfonsi, M.; Althueser, L.; Amaro, F.D.; Anthony, M.; Arneodo, F.; Baudis, L.; Bauermeister, B.; et al. Dark Matter Search Results from a One Ton-Year Exposure of XENON1T. *Phys. Rev. Lett.* **2018**, *121*, 111302. [[CrossRef](#)]
31. Akerib, D.S.; Akerlof, C.W.; Alsum, S.K.; Araújo, H.M.; Arthurs, M.; Bai, X.; Bailey, A.J.; Balajthy, J.; Balashov, S.; Bauer, D.; et al. Projected WIMP sensitivity of the LUX-ZEPLIN dark matter experiment. *Phys. Rev. D* **2020**, *101*, 052002. [[CrossRef](#)]
32. Aalbers, J.; Akerib, D.S.; Akerlof, C.W.; Al Musalhi, A.K.; Alder, F.; Alqahtani, A.; Alsum, S.K.; Amarasinghe, C.S.; Ames, A.; Anderson, T.J.; et al. First Dark Matter Search Results from the LUX-ZEPLIN (LZ) Experiment. *arXiv* **2022**, arXiv:2207.03764.
33. Ellis, J.R.; Falk, T.; Olive, K.A. Neutralino-Stau coannihilation and the cosmological upper limit on the mass of the lightest supersymmetric particle. *Phys. Lett. B* **1998**, *444*, 367–372. [[CrossRef](#)]
34. Boehm, C.; Djouadi, A.; Drees, M. Light scalar top quarks and supersymmetric dark matter. *Phys. Rev. D* **2000**, *62*, 035012. [[CrossRef](#)]
35. Baer, H.; Krupovnickas, T.; Mustafayev, A.; Park, E.K.; Profumo, S.; Tata, X. Exploring the BWCA (bino-wino co-annihilation) scenario for neutralino dark matter. *J. High Energy Phys.* **2005**, *12*, 011. [[CrossRef](#)]
36. Badziak, M.; Nałecz, I. First-order phase transitions in Twin Higgs models. *arXiv* **2022**, arXiv:2212.09776.
37. Abbiendi, G.; Ainsley, C.; Akesson, P.F.; Alexander, G.; Allison, J.; Amaral, P.; Anagnostou, G.; Anderson, K.J.; Arcelli, S.; Asai, S.; et al. Search for anomalous production of dilepton events with missing transverse momentum in e^+e^- collisions at $s^{*}(1/2) = 183\text{-GeV}$ to 209-GeV . *Eur. Phys. J. C* **2004**, *32*, 453–473. [[CrossRef](#)]

38. Heister, A.; Schael, S.; Barate, R.; Bruneliere, R.; Bonis, I.D.; Decamp, D.; Goy, C.; Jezequel, S.; Lees, J.P.; Martin, F.; et al. Search for scalar leptons in e^+e^- collisions at center-of-mass energies up to 209-GeV. *Phys. Lett. B* **2002**, *526*, 206–220. [[CrossRef](#)]
39. Abdallah, J.; Abreu, P.; Adam, W.; Adzic, P.; Albrecht, T.; Alderweireld, T.; Alemany-Fernandez, R.; Allmendinger, T.; Allport, P.P.; Amaldi, U.; et al. Searches for supersymmetric particles in e^+e^- collisions up to 208-GeV and interpretation of the results within the MSSM. *Eur. Phys. J. C* **2003**, *31*, 421–479. [[CrossRef](#)]
40. Achard, P.; Adriani, O.; Aguilar-Benitez, M.; Alcaraz, J.; Alemanni, G.; Allaby, J.; Aloisio, A.; Alviggi, M.G.; Anderhub, H.; Andreev, V.P.; et al. Search for scalar leptons and scalar quarks at LEP. *Phys. Lett. B* **2004**, *580*, 37–49. [[CrossRef](#)]
41. Search for direct pair production of supersymmetric partners of τ leptons in the final state with two hadronically decaying τ leptons and missing transverse momentum in proton-proton collisions at $\sqrt{s} = 13$ TeV. *arXiv* **2022**, arXiv:2207.02254.
42. Belanger, G.; Boudjema, F.; Pukhov, A.; Semenov, A. MicrOMEGAs: A Program for calculating the relic density in the MSSM. *Comput. Phys. Commun.* **2002**, *149*, 103–120. [[CrossRef](#)]
43. Bélanger, G.; Boudjema, F.; Pukhov, A.; Semenov, A. micrOMEGAs: Version 1.3. *Comput. Phys. Commun.* **2006**, *174*, 577–604. [[CrossRef](#)]
44. Belanger, G.; Boudjema, F.; Pukhov, A.; Semenov, A. MicrOMEGAs 2.0: A Program to calculate the relic density of dark matter in a generic model. *Comput. Phys. Commun.* **2007**, *176*, 367–382. [[CrossRef](#)]
45. Belanger, G.; Boudjema, F.; Pukhov, A.; Semenov, A. micrOMEGAs_3: A program for calculating dark matter observables. *Comput. Phys. Commun.* **2014**, *185*, 960–985. [[CrossRef](#)]
46. Badziak, M.; Delgado, A.; Olechowski, M.; Pokorski, S.; Sakurai, K. Detecting underabundant neutralinos. *J. High Energy Phys.* **2015**, *11*, 053. [[CrossRef](#)]
47. Agrawal, P.; Cyr-Racine, F.Y.; Randall, L.; Scholtz, J. Make Dark Matter Charged Again. *J. Cosmol. Astropart. Phys.* **2017**, *05*, 022. [[CrossRef](#)]
48. Evans, J.A.; Shelton, J. Long-Lived Staus and Displaced Leptons at the LHC. *J. High Energy Phys.* **2016**, *04*, 056. [[CrossRef](#)]
49. Sirunyan, A.M.; Tumasyan, A.; Adam, W.; Ambroggi, F.; Asilar, E.; Bergauer, T.; Brandstetter, J.; Brondolin, E.; Dragicevic, M.; Erö, J.; et al. Search for disappearing tracks as a signature of new long-lived particles in proton-proton collisions at $\sqrt{s} = 13$ TeV. *J. High Energy Phys.* **2018**, *08*, 16. [[CrossRef](#)]
50. Aaboud, M.; Aad, G.; Abbott, B.; Abbott, D.C.; Abidinov, O.; Abeloos, B.; Abhayasinghe, D.K.; Abidi, S.H.; AbouZeid, O.S.; Abraham, N.L.; et al. Search for heavy charged long-lived particles in the ATLAS detector in 36.1 fb^{-1} of proton-proton collision data at $\sqrt{s} = 13$ TeV. *Phys. Rev. D* **2019**, *99*, 092007. [[CrossRef](#)]

Disclaimer/Publisher’s Note: The statements, opinions and data contained in all publications are solely those of the individual author(s) and contributor(s) and not of MDPI and/or the editor(s). MDPI and/or the editor(s) disclaim responsibility for any injury to people or property resulting from any ideas, methods, instructions or products referred to in the content.